



HAL
open science

STDP Plasticity in TRN Within Hierarchical Spike Timing Model of Visual Information Processing

Petia Koprinkova-Hristova, Nadejda Bocheva, Simona Nedelcheva, Miroslava Stefanova, Bilyana Genova, Radoslava Krалеva, Velin Krалev

► To cite this version:

Petia Koprinkova-Hristova, Nadejda Bocheva, Simona Nedelcheva, Miroslava Stefanova, Bilyana Genova, et al.. STDP Plasticity in TRN Within Hierarchical Spike Timing Model of Visual Information Processing. 16th IFIP International Conference on Artificial Intelligence Applications and Innovations (AIAI), Jun 2020, Neos Marmaras, Greece. pp.279-290, 10.1007/978-3-030-49161-1_24. hal-04050609

HAL Id: hal-04050609

<https://inria.hal.science/hal-04050609>

Submitted on 29 Mar 2023

HAL is a multi-disciplinary open access archive for the deposit and dissemination of scientific research documents, whether they are published or not. The documents may come from teaching and research institutions in France or abroad, or from public or private research centers.

L'archive ouverte pluridisciplinaire **HAL**, est destinée au dépôt et à la diffusion de documents scientifiques de niveau recherche, publiés ou non, émanant des établissements d'enseignement et de recherche français ou étrangers, des laboratoires publics ou privés.



Distributed under a Creative Commons Attribution 4.0 International License

STDP Plasticity in TRN within Hierarchical Spike Timing Model of Visual Information Processing*

Petia Koprinkova-Hristova¹[0000-0002-0447-9667], Nadejda Bocheva²[0000-0001-7792-7742], Simona Nedelcheva¹, Miroslava Stefanova², Bilyana Genova², Radoslava Kraleva³[0000-0003-3322-7298], and Velin Kralev³[0000-0002-7780-8281]

¹ Institute of Information and Communication Technologies, Bulgarian Academy of Sciences, Sofia, Bulgaria

pkoprinkova@bas.bg, croft883@gmail.com

² Institute of Neurobiology, Bulgarian Academy of Sciences, Sofia, Bulgaria
nadya@percept.bas.bg, mirad_st@abv.bg, b.genova@abv.bg

³ Department of Informatics, South West University, Blagoevgrad, Bulgaria
rady_kraleva@swu.bg, velin_kralev@swu.bg

Abstract. We investigated age related synaptic plasticity in thalamic reticular nucleus (TRN) as a part of visual information processing system in the brain. Simulation experiments were performed using a hierarchical spike timing neural network model in NEST simulator. The model consists of multiple layers starting with retinal photoreceptors through thalamic relay, primary visual cortex layers up to the lateral intraparietal cortex (LIP) responsible for decision making and preparation of motor response. All synaptic inter- and intra-layer connections of our model are structured according to the literature information. The present work extends the model with spike timing dependent plastic (STDP) synapses within TRN as well as from visual cortex to LIP area. Synaptic strength changes were forced by teaching signal typical for three different age groups (young, middle and elderly) determined experimentally from eye movement data collected by eye tracking device from human subjects performing a simplified simulated visual navigation task.

Keywords: Spike timing neural model · Spike timing dependent plasticity · Visual system · Decision making · Saccade generation.

1 Introduction

The visual information coming through our eyes is processed by a hierarchy of multiple consecutive brain areas having different functionality. The sensory layer (retina) consists of photo-receptive cells. It transforms the incoming light into

* This work was financially supported by the Bulgarian Science Fund, grant No DN02-3-2016 "Modeling of voluntary saccadic eye movements during decision making".

electrical signals fed into the brain via retina ganglion cells (RGC). Next a relay structure (lateral geniculate nucleus (LGN) and thalamic reticular nucleus (TRN)) transmits the signals to the primary visual cortex (V1). Higher brain areas (middle temporal area (MT) and medial superior temporal area (MST)) are responsible for motion information processing. Based on perceived sensory information our brain makes decisions and initiates motor responses. The decisions based on processed visual information are taken in the lateral intraparietal area (LIP) that is also responsible for preparation of the eyes' motor response (change of gaze direction) called saccade. Most of the existing motion information processing models are restricted to the interactions between some of the mentioned areas like: V1 and MT in [25, 1, 2, 5], V1, MT and MST in [21]; MT and MST in [9, 19]. Many models consider only the feedforward interactions (e.g. [25, 26]) disregarding the feedback connectivity; others employ rate-based equations (e.g. [20, 10]) considering an average number of spikes in a population of neurons. In our preliminary research [11] we have developed and implemented in NEST 2.12.0 simulator ([16]) a spike-timing neural network model having static inter- and intra-layer synaptic connections structured according to the literature information that includes all mentioned above structures. Determination of the parameters' values for such kind of models is usually done using electrophysiological recordings directly from the brain that are rarely available for all modelled brain areas for human subjects. Our preliminary attempt to tune the synaptic connections between the last two layers (MST and LIP) using final outcome from experiments on visual information perception and decision making, i.e. recorded motor reaction (saccade generation) revealed that spike timing dependent plasticity (STDP) led to age-related changes in these synaptic weights [12]. Training data was collected from the human decisions during experiment with visual stimuli simulating optic flow patterns of forward self-motion on a linear trajectory to the left or to the right of the center of the visual field with a gaze in the direction of heading. The subjects had to indicate the perceived direction of heading by saccade movement. The mean latency of the eye movements for each one of the three age groups (young, middle age and elderly) was used as training signal fed into the output layer of the model structures.

In the present work we extended our model [11] with feedback connectivity between each pair of consecutive layers thus allowing for complete feedback propagation of training signals. We also allow STDP plasticity in the feedback / feedforward connections within thalamic relay structure in order to test whether training signal propagates deeper in the model. The thalamus provides sensory input to the cortex, but it also receives feedback from the cortex that is considered to be modulatory [24]. It receives also indirect inhibitory feedback from TRN, a structure that is considered to be related to attention (e.g., [6]) and thus, it is also expected to have a modulatory effect on the activity in the thalamus. Hence, a propagation of the effects of training to the thalamus would support the biological relevance of the proposed model. The paper is organized as follows: section 2 describes briefly the overall model structure and parameters; next we describe briefly the experimental set-up and data processing; section 4 presents

results from STDP training of the model and obtained parameters typical for mean behaviour of each one of the three tested age groups; the concluding section comments obtained results and determines directions for our future work.

2 Model Structure

The hierarchical model organization is shown on Fig. 1. It is based on structure developed first in [11] based on literature information about each layer neurons' functionality, structure and connectivity according to [7, 8, 15, 17, 18, 23, 27]. The difference is in additional feedback connections from MST to MT as well as STDP connections within thalamic relay (to and from LGN to TRN and interneurons IN) and from MST to LIP area.

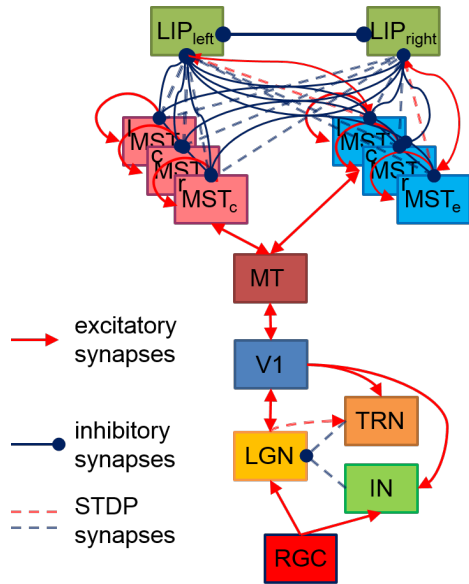


Fig. 1. Model structure.

Detailed description of model structure and connectivity design can be found in [11]. Here we briefly explain it. Each coloured rectangle on Fig. 1 represents a layer of neurons positioned on a regular two-dimensional grid. Connections between layers are denoted by arrows having color corresponding to the sign of their weights (red for positive, called excitatory and blue for negative, called inhibitory connections respectively). Connections denoted by solid lines have constant weights while those denoted by dashed lines are able to change their weights in dependence on activity of pre- and postsynaptic neurons, i.e. they have spike timing dependent plasticity (STDP) [22]. Sensory layer (RGC) as well as

thalamic relay (LGN) consist of two sub-layers of neurons reacting positively (ON1 and ON2) and negatively (OFF1 and OFF2) to the increase of luminosity. Each neuron within LGN has its own interneuron (IN) and thalamic reticular nucleus (TRN) that processes feedback from the next (V1) layer. Layers V1 and MT have identical structure and connectivity adopted from [15] that makes them sensitive to orientation and direction of movement of visual objects. The MST consists of two layers, sensitive to expansion (MSTe) and contraction (MSTc) movement patterns respectively, like in [17]. These sub-structures are represented as three groups on Fig. 1 that are able to detect expansion or contraction of moving objects from imaginary centers positioned left, right or at the center of the visual scene denoted by l, r and c on Fig. 1. Since our model aims to decide whether the expansion center of a moving dot stimulus is left or right from the stimulus center, we proposed a task-dependent design of excitatory/inhibitory connections from MST expansion/contraction layers to the two LIP sub-regions whose increased firing rate corresponds to two taken decisions for two alternative motor responses - eye movement to the left or to the right.

The reaction of RGC to light changes is simulated by a convolution with a spatio-temporal filter following model from [27]. For the neurons in LGN conductance-based leaky integrate-and-fire neuron model as in [4] (*iaf_chzk_2008* in NEST) was adopted. For the rest of neurons, leaky integrate-and-fire model with exponential shaped postsynaptic currents according to [28] (*iaf_psc_exp* in NEST) was used. All connection parameters are the same as in the cited literature sources.

3 Experimental Set-up

3.1 Behavioral experiment and data collection

The time series data used to test the idea described above were collected by eye tracking device that recorded the human eye movements during a behavioral experiment performed with the participation of volunteer human subjects responding to series of visual stimuli. Detailed description of experimental conditions can be found in [3, 13].

Here we briefly remind basic experimental set-up. The visual stimulation was performed by projection on a gray screen of different patterns of 50 white moving dots in a circular aperture with radius of 7.5 cm positioned in the middle of a computer screen. The patterns of dot movements were designed to mimic dots expansion from an imaginary center positioned left or right from the screen center respectively. The subject sat at 57cm from the monitor screen. Each stimulus presentation was preceded by a warning sound signal. A red fixation point with size of 0.8cm appeared in the center of the screen for 500 ms. The stimuli were presented immediately after the disappearance of the fixation point. The Subject’s task was to continue looking at the position where the fixation point was presented until he/she made a decision where the center of the pattern was and to indicate this position by a saccade (fast eye movement). The subjects also had to press the left or the right mouse button depending on the perceived

position of the center - to the left or to the right from the middle of the screen. If the subject could not make a decision during the stimulus presentation (3.3 s for 100 consecutive frames), the stimulus disappeared and the screen remained gray until the subject made a response. Each experimental session consisted of consecutive presentation in random order of 10 patterns for each of the 14 possible stimulus types from chosen experimental condition, i.e. totally 140 stimuli were observed by test subjects during every session. The eye movements of the participants in the experiment were recorded by a specialized hardware – Jazz novo eye tracking system [30]. All recordings from all the sensors of the device for one session per person were collected with 1 KHz frequency and the information is stored in files. These include: the calibration information; records of horizontal and vertical eye positions in degrees of visual angle eye_x and eye_y ; screen sensor signal for presence/absence of a stimulus on the monitor; microphone signal recording sounds during the experiment; information about tested subjects (code) and type of the experimental trial for each particular record.

Three age groups took part in the experiment: young (between 20 and 34 years old), elderly (from 57 to 84 years old) and middle aged group (between 36 and 52 years old). All participants have given a written informed consent for participating in the study after explanation of the experimental procedure. The experiments were approved by the ethical committee of the Institute of Neurobiology, Bulgarian Academy of Sciences and are in accordance with the Declaration of Helsinki.

3.2 Data processing

The raw data was collected in a relational database [14]. It allowed us to process all sensors data in order to extract only the records from the presentation of a stimulus on the screen to the mouse button press. The data between the stimulus presentations were excluded since it is not relevant to the eye movements during task performance. The processed eye movement data were refined by removing the outliers and a drift diffusion model of mean response time of each one of the age groups for all four experimental conditions was derived [3].

Based on the identified mean reaction times from [3] we've created training signals as generating currents I_{left} and I_{right} for the left and right LIP neurons respectively as follows:

$$I_{left/right} = A_{left/right} / (1 + \exp(k_{left/right}t)) \quad (1)$$

Amplitude $A_{left/right}$ defines maximal input current (in pA) while $k_{left/right}$ determines settling time of the exponent that corresponds to the mean reaction time determined from experiments for each age group and experimental condition. For all three age groups amplitude values were the same: $A_{left} = 200$ and $A_{right} = 100$. In order to achieve approximately the settling time determined from experimental data, parameter $k_{left/right}$ has different values for three age groups (Y - young, M - middle, O - old) with opposite signs for left and right case

of stimulus respectively as follows: $k_{left/right}^Y = -/+0.02$; $k_{left/right}^M = -/+0.01$; $k_{left/right}^O = -/+0.005$.

4 Simulations

The overall model was tested using visual stimulation simulating an observer's motion on a linear trajectory with eyes fixed in the heading direction. Example from the stimuli used in the behavioural study with a position of the imaginary center to the left was selected so our aim is to teach the model to react correctly with increased spiking activity in the left LIP area after a time interval typical for group mean reaction time for each age. Training was performed in iterations, each one consisting of presentation of visual stimulation to the model input and the teaching signal to its output layer respectively.

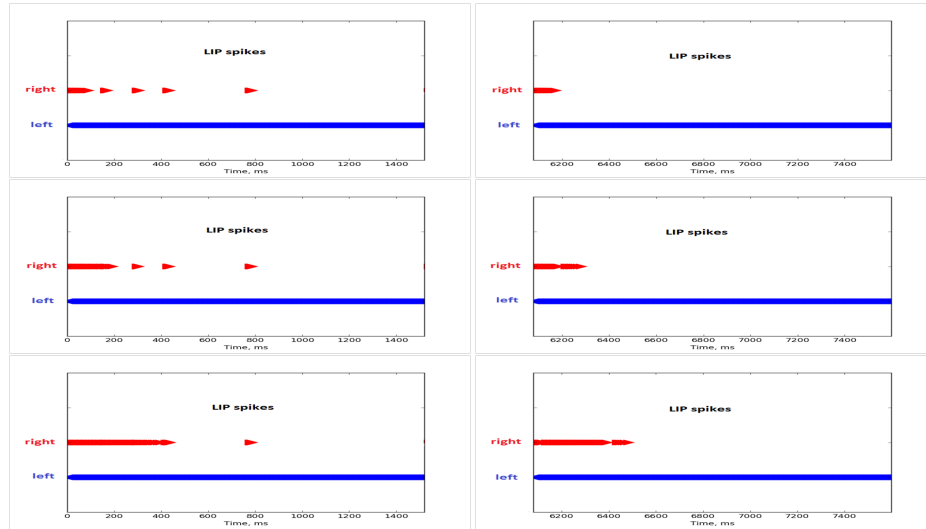


Fig. 2. LIP reactions for left (blue arrows) and right (red arrows) during first (left column) and fifth (right column) iteration for three age groups (top - young, second row - middle age and bottom row - elderly people).

Fig. 2 presents spikes in both left (blue) and right (red) LIP layers obtained during first and last (fifth) iteration. It shows that the frequency of spikes induced in the right LIP layer decrease with time and after a varying delay for the three age groups no more spikes occur. The frequency of spikes for the left LIP region increases with time (though this change is not evident from the figure). Fig. 3 compares the weights of connections from MST to LIP area obtained after five iterations for the three age groups. For clarity only weights that are different for the three age groups are shown. The connections from expansion template

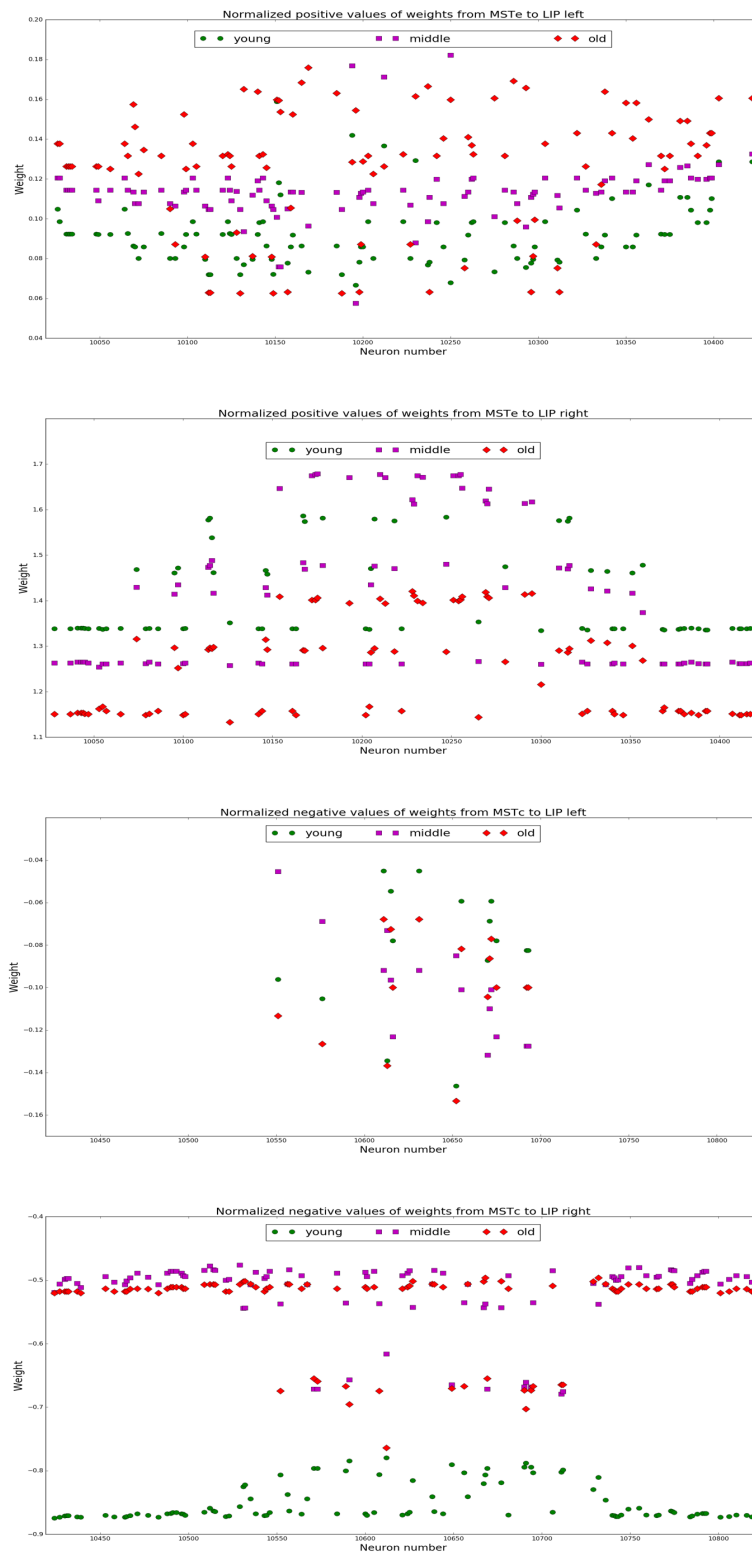


Fig. 3. Connections from MST to LIP.

Table 1. Mean values of normalized connection weights from MST to LIP.

It.	MSTe to LIP left			MSTe to LIP right			MSTc to LIP left			MSTc to LIP right		
	<i>Y</i>	<i>M</i>	<i>O</i>	<i>Y</i>	<i>M</i>	<i>O</i>	<i>Y</i>	<i>M</i>	<i>O</i>	<i>Y</i>	<i>M</i>	<i>O</i>
1	+0.08	+0.13	+0.10	+1.48	+1.40	+1.25	-0.95	-0.95	-0.95	-0.99	-0.99	-0.99
2	+0.12	+0.10	+0.12	+1.48	+1.40	+1.25	-0.95	-0.95	-0.95	-1.05	-1.04	-0.89
5	+0.09	+0.11	+0.13	+1.48	+1.40	+1.25	-0.95	-0.95	-0.95	-0.95	-0.83	-0.84

Table 2. Variances of normalized connection weights from MST to LIP.

It.	MSTe to LIP left [E^{-4}]			MSTe to LIP right [E^{-2}]			MSTc to LIP left [E^{-2}]			MSTc to LIP right [E^{-2}]		
	<i>Y</i>	<i>M</i>	<i>O</i>	<i>Y</i>	<i>M</i>	<i>O</i>	<i>Y</i>	<i>M</i>	<i>O</i>	<i>Y</i>	<i>M</i>	<i>O</i>
1	2.03	2.21	2.27	2.53	2.50	1.06	4.02	3.86	3.87	0.00	0.00	0.00
2	6.89	9.09	7.63	2.53	2.50	1.06	4.02	3.86	3.87	0.44	0.38	2.35
5	2.52	2.27	9.55	2.53	2.50	1.06	4.02	3.86	3.87	0.52	5.35	4.96

area of MST are of both types (excitatory and inhibitory) in dependence on their focal points position. Our simulations revealed that STDP rule changes only the positive connection weights while the negative ones remained constant. For the contraction MST layer connections to both LIP areas are inhibitory and they were changed more significantly for the right (incorrect) LIP area. Hence, it appears that the activity in the LIP layers is not directly related to the weights of the connections for the MST templates that correspond to the stimulus (i.e. the MSTe), but it depends on the combined activity of all templates.

Fig. 3 and Tables 1 and 2 show the connection weight changes after iterative training. We observe that the clearest differentiation that remains stable during iterations is in the excitatory connections from the expansion MST layer to the right LIP area. These connections' weights became smaller for the elderly group and bigger for the group of young test subjects while the excitatory connections from MSTe to the left LIP area (corresponding to correct response in this case) as well the inhibitory connections from MSTc to right (incorrect) LIP area reach highest absolute values for elderly group and lowest for the group of young test subjects. Therefore, the reduction in LIP activity in the wrong LIP layer is achieved by different means for the young and the elderly group suggesting a re-organization and different balance between the excitatory and inhibitory connections between the different layers and areas.

We also investigated connection weight changes during iterative training in TRN and LGN. Most of the connections within thalamic relay remained constant. The only observed changes were in the inhibitory feedback connections from TRN to LGN. This result implies an indirect modulatory effect of the activity in LGN from the cortical regions. The values obtained after five training iterations are shown on Fig. 4. Mean values and variances of trained weights obtained after one, two and five iterations for teaching signals corresponding to

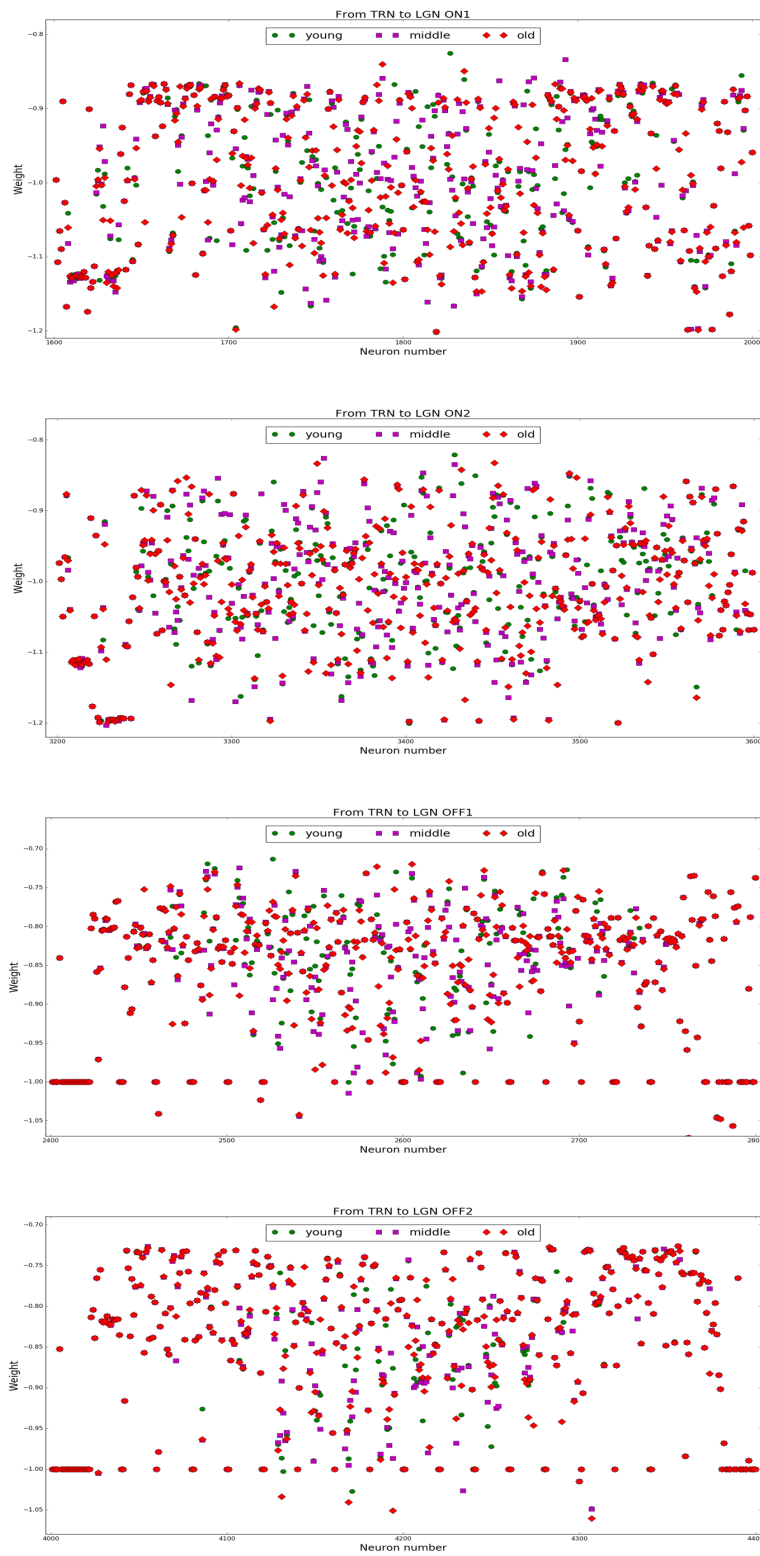


Fig. 4. Connections from TRN to LGN.

Table 3. Mean values of normalized connection weights from TRN to LGN.

It.	TRN to LGN ON1			TRN to LGN ON2			TRN to LGN OFF1			TRN to LGN OFF2		
	<i>Y</i>	<i>M</i>	<i>O</i>	<i>Y</i>	<i>M</i>	<i>O</i>	<i>Y</i>	<i>M</i>	<i>O</i>	<i>Y</i>	<i>M</i>	<i>O</i>
1	-0.98	-0.98	-0.98	-0.97	-0.97	-0.97	-0.87	-0.87	-0.87	-0.85	-0.85	-0.85
2	-0.98	-0.98	-0.98	-1.01	-1.01	-1.01	-0.86	-0.86	-0.86	-0.84	-0.84	-0.84
5	-0.99	-0.99	-0.99	-1.01	-1.01	-1.01	-0.86	-0.86	-0.86	-0.84	-0.84	-0.84

Table 4. Variances of normalized connection weights from TRN to LGN.

It.	TRN to LGN ON1 [E^{-3}]			TRN to LGN ON2 [E^{-3}]			TRN to LGN OFF1 [E^{-3}]			TRN to LGN OFF2 [E^{-3}]		
	<i>Y</i>	<i>M</i>	<i>O</i>	<i>Y</i>	<i>M</i>	<i>O</i>	<i>Y</i>	<i>M</i>	<i>O</i>	<i>Y</i>	<i>M</i>	<i>O</i>
1	5.31	5.31	5.31	4.67	4.67	4.67	6.35	6.35	6.35	7.72	7.72	7.72
2	3.30	3.30	3.39	6.26	6.26	6.07	6.28	6.28	6.45	8.71	8.71	8.64
5	8.94	9.03	8.92	7.00	7.45	6.96	7.09	6.94	6.96	8.68	8.59	8.57

the three age groups are presented in Tables 3 and 4 respectively. While the connections from MST to LIP for the three age groups start to diverge just after the first iteration, those in thalamic relay needed more than two iterations to differentiate.

Concerning the propagation of learning-induced signal to the thalamic relay, the observed greater strength of the connections from TRN for the ON responses than to the OFF ones might be considered as an improvement of the sensitivity to the luminance changes in the stimulus and improved signal to noise ratio in its encoding at initial stages of the visual information processing. The increased variability of the connections might be related to the spatial distribution of the dots in the stimulus and to the greater specificity to it induced by the inhibitory connections from TRN to LGN. In the deeper STDP connectivity in thalamic relay, age differentiation became obvious after fifth iteration. Besides, after second iteration connectivity for young and middle age groups remain identical and different from the elderly group, while after the fifth iteration it seems that the middle age group differs from both young and elderly groups who became a little bit closer. This result suggests learning-induced plasticity that can alleviate the negative effect of ageing though after longer training periods.

5 Conclusions

In conclusion, the attempt to train our hierarchical spike timing neural network model using training signal for only output layer that is based on human reaction time from behavioural experiments rather than on electrophysiological recordings from the brain, revealed that it is completely possible to change not only connectivity between the last two layers of the model but also to propagate the teaching signal much deeper in the hierarchical structure. Such feedback mod-

ulatory propagation from the cortical areas to the thalamus is in accordance with the known physiological data and gives credit to our modeling efforts. Our preliminary results also revealed typical for aging differentiation of connection weights especially for the connections between MST and LIP areas. While for all age groups the activity in the LIP layer corresponding to the incorrect response terminates with time, this effect is achieved by different recombination of the connection weights for the different age groups. Concerning deep thalamic relay, although age-related changes propagate much slowly, they were also observed after more training iterations indicating that learning-induced activity may reduce the age-related changes induced by the imbalance of inhibitory and excitatory activity in the cortical regions.

Further direction of our investigations will be enriching our hierarchical model with more STDP connections in order to complete training of its connection weights in dependence on typical reactions of different age groups.

References

1. Bayerl, P., Neumann, H.: Disambiguating visual motion through contextual feedback modulation. *Neural Computation*, **16**(10), 2041–2066 (2004)
2. Bayerl, P.: A Model of Visual Perception, PhD Thesis, Ulm University, Germany (2005)
3. Bocheva, N., Genova, B., Stefanova, M.: Drift diffusion modeling of response time in heading estimation based on motion and form cues. *Int. J. of Biology and Biomedical Engineering*, **12**, 75–83 (2018)
4. Casti, A., Hayot, F., Xiao, Y., Kaplan, E.: A simple model of retina-LGN transmission. *J. Comput. Neurosci.*, **24**, 235–252 (2008)
5. Chessa, M., Sabatini, S., Solari, F.: A systematic analysis of a V1–MT neural model for motion estimation. *Neurocomputing*, **173**, 1811–1823 (2016)
6. Crick, F.: Function of the thalamic reticular complex: The searchlight hypothesis. *Proceedings of the National Academy of Sciences USA*, **81**, 4586–4590 (1984)
7. Escobar, M.-J., Masson, G. S., Vieville, T., Kornprobst, P.: Action recognition using a bio-inspired feedforward spiking network. *Int. J. Comput. Vis.*, **82**, 284–301 (2009)
8. Ghodrati, M., Khaligh-Razavic, S.-M., Lehky, S. R.: Towards building a more complex view of the lateral geniculate nucleus: Recent advances in understanding its role. *Progress in Neurobiology*, **156**, 214–255 (2017)
9. Grossberg, S., Mingolla, E., Pack, C.: A neural model of motion processing and visual navigation by cortical area MST. *Cerebral Cortex*, **9**(8), 878–895 (1999)
10. Grossberg, S., Mingolla, E., Viswanathan, L.: Neural dynamics of motion integration and segmentation within and across apertures. *Vision Research*, **41**(19), 2521–2553 (2001)
11. Koprinkova-Hristova, P., Bocheva, N., Nedelcheva, S., Stefanova, M.: Spike timing neural model of motion perception and decision making. *Frontiers in Computational Neuroscience*, **13**, art. no. 20 (2019). <https://doi.org/10.3389/fncom.2019.00020>
12. Koprinkova-Hristova, P., Nedelcheva, S., Bocheva, N., Krалева, R., Krалев, V., Stefanova, M., Genova, B.: STDP training of hierarchical spike timing model of visual information processing. In: World Congress on Computational Intelligence 2020 (accepted).

13. Koprinkova-Hristova, P., Stefanova, M., Genova, B. et al. Features extraction from human eye movements via echo state network. *Neural Comput. and Applic.* (2019). <https://doi.org/10.1007/s00521-019-04329-z>
14. Kraveva, R., Kravev, V., Sinyagina, N., Koprinkova-Hristova, P., Bocheva, N.: Design and analysis of a relational database for behavioral experiments data processing. *International Journal of Online Engineering*, **14**(2), 117–132 (2018)
15. Kremkow, J., Perrinet, L. U., Monier, C., Alonso, J.-M., Aertsen, A., Fregnac, Y., Masson, G. S.: Push-pull receptive field organization and synaptic depression: Mechanisms for reliably encoding naturalistic stimuli in V1. *Frontiers in Neural Circuits*, **10** (2016). <https://doi.org/10.3389/fncir.2016.00037>
16. Kunkel, S. et al., NEST 2.12.0. Zenodo (2017). <https://doi.org/10.5281/zenodo.259534>
17. Layton, O. W., Fajen, B. R.: Possible role for recurrent interactions between expansion and contraction cells in MSTd during self-motion perception in dynamic environments. *Journal of Vision*, **17**(5), 1–21 (2017)
18. Nedelcheva, S., Koprinkova-Hristova, P.: Orientation selectivity tuning of a spike timing neural network model of the first layer of the human visual cortex. In: *Advanced Computing in Industrial Mathematics*, K. Georgiev, M. Todorov, and I. Georgiev (Eds.), *Studies in Computational Intelligence*, vol. 793, pp. 291–303, (2019)
19. Perrone, J.: A neural-based code for computing image velocity from small sets of middle temporal (MT/V5) neuron inputs. *Journal of Vision*, **12**(8) (2012). <https://doi.org/10.1167/12.8.1>
20. Raudies, F., Neumann, H.: A neural model of the temporal dynamics of figure-ground segregation in motion perception. *Neural Networks*, **23**(2), 160–176 (2010)
21. Raudies, F., Mingolla, E., Neumann, H.: Active gaze control improves optic flow-based segmentation and steering. *PLoS ONE*, **7**(6), 1–19 (2012)
22. Rubin, J., Lee, D., Sompolinsky, H.: Equilibrium properties of temporally asymmetric Hebbian plasticity. *Physical Review Letters*, **86**, 364–367 (2001)
23. Sadeh, S., Rotter, S.: Statistics and geometry of orientation selectivity in primary visual cortex. *Biol. Cybern.*, **108**, 631–653 (2014)
24. Sherman, S. M., Guillery, R. W.: *Exploring the thalamus and its role in cortical function* (2d ed.). Cambridge, MA: MIT Press (2009)
25. Simoncelli, E., Heeger, D.: A model of neuronal responses in visual area MT. *Vision Research*, **38**, 743–761 (1998)
26. Solari, F., Chessa, M., Medathati, K., Kornprobst, P.: What can we expect from a V1-MT feedforward architecture for optical flow estimation?. *Signal Processing: Image Communication*, **39**, Part B, 342–354 (2015)
27. Troyer, T. W., Krukowski, A. E., Priebe, N. J., Miller, K. D.: Contrast invariant orientation tuning in cat visual cortex: thalamocortical input tuning and correlation-based intracortical connectivity. *J. Neurosci.*, **18**, 5908–5927 (1998)
28. Tsodyks, M., Uziel, A., Markram, H.: Synchrony generation in recurrent networks with frequency-dependent synapse. *The Journal of Neuroscience*, **20**(RC50), 1–5 (2000)
29. Webb, B. S., Ledgeway, T.Y., McGraw, P. V.: Relating spatial and temporal orientation pooling to population decoding solutions in human vision. *Vision Research*, **50**, 2274–2283 (2010)
30. <http://www.ober-consulting.com/product/jazz/>